Proceedings of the ASME 2024
International Design Engineering Technical Conferences and
Computers and Information in Engineering Conference
IDETC-CIE2024
August 25-28, 2024, Washington, DC

DETC2024-146264

DYNAMIC STATE TRACKING OF OVERHEAD POWERLINES WITH REAL TIME STATE ESTIMATION: A DATA-DRIVEN APPROACH

Nipun Remasan Nambiar[1,†,*], Oumar Barry[2,*]

[1]Virginia Polytechnic Institute and State University Blacksburg, VA
[2]Virginia Polytechnic Institute and State University Blacksburg, VA

ABSTRACT

This study focuses on laying the groundwork for the effective vibration suppression of power lines using mobile damping robots (MDR). Earlier research shows that effective vibration suppression is achieved by positioning the MDR at the anti-nodes of the power line. This study focuses on accurately estimating the dynamic state of the power line using a data-driven approach, hence identifying the position of the antinode. The entire dynamics of the vibration of the system is estimated from the displacement data of the power line using Dynamic Mode Decomposition (DMD) and the resulting system is stabilized with Tikhonov Regularization. The stabilized system is then used in conjunction with a Kalman Filter to accurately estimate the dynamic state of the power line using minimal displacement. All displacement data used in this study is acquired from a Galerkin model of the power line. This study shows that this method is a viable alternative to existing numerical methods which are often computationally expensive and time-consuming.

Keywords: Vibration Control, State-Estimation, Data-Driven modeling, Kalman Filter

NOMENCLATURE

Powerline

y	Transverse Displacement $[m]$
f_0	Amplitude of forcing function $[N]$
ω_e	Excitation Frequency $[rad\ s^{-1}]$
δ	Dirac-delta function

Dynamic Mode Decomposition

m	Order of the time series
k	Time-step
A	State Transition Matrix
λ	Eigenvalue
r	Number of modes
α	Tikhonov Regularization Parameter

1. INTRODUCTION

Wind-induced vibrations (WIV) is one of the major causes responsible for the failure of power-transmission lines. These WIVs cause the repetitive cycles of bending stress in powerlines and eventually resulting in failure, [1–4]. The failure of powerlines not only causes discomfort in daily-life, but also responsible for significant financial loss to power industry. Therefore, it is necessary to develop an efficient method to suppress these unwanted WIVs of powerlines. This is the focus of the current work.

One of the methods to suppress the WIVs is the use of Fixed passive vibration absorbers (FPVAs) [5, 6]. However, FPVAs are not efficient because of their fixed optimal location for a given mode. Further, a FPVA might also contribute in the fatigue failure of the powerline due to the added strain from the mass of the FPVA, [7].

It has been well established that vibration absorbers are most effective when they are positioned at the antinode of the vibration loop, i.e., the point of highest amplitude of vibration [8]. Therefore, to overcome the above-mentioned limitation of the FPVA, a mobile absorber in the form of a mobile damping robot (MDR) was proposed in [9, 10]. Since the MDR is capable of traversing along the span of the power line, it can move to the point of antinode and hence, suppress WIVs effectively. We emphasize that although there are other mobile robots that exist in the literature, they are more focused on inspection, are expensive, and unsuitable for long-term mounting on the power line due to their heavy mass. These shortcomings can be overcome by the proper design of MDR.

As mentioned earlier, the effective vibration suppression of the powerline is achieved by mounting the vibration absorber at the anti-node. Hence, for optimum performance of MDR, information about the position of the antinode is required in real

[†]Joint first authors
[*]Corresponding author: barry@vt.edu
Documentation for `asmeconf.cls`: Version 1.37, May 27, 2024.

FIGURE 1: Conceptual design model of the mobile damping robot

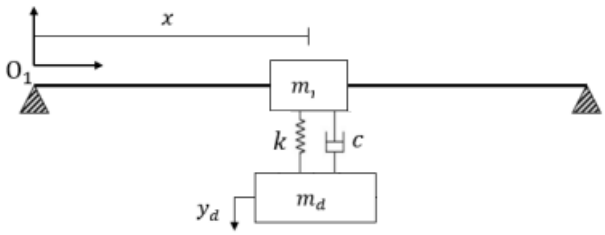

FIGURE 2: Schematic of the power line with MDR

time. Though this can be achieved to some degree using numerical methods, it is a computationally intensive and expensive process. Also, the data related to anti-node cannot be accessible to MDR in real time. Hence we resort to data-driven methods. Data-driven methods have gained popularity in recent years owing to their ability to extract valuable insights and build low-dimensional models from complex systems directly from data. From data, these methods can capture the inherent characteristics and behaviors of a system, even when the underlying physics is not fully understood.

2. MATHEMATICAL MODELING

The schematic of the power line with MDR is shown in Fig 2. In the current work, the power line is modeled as an Euler-Bernoulli beam, while the MDR is modeled as a spring-mass-damper system [11]. The horizontal displacement is defined as zero and self-damping is ignored as it is considered to have negligible effects. The power line parameters are shown in Table 1.

Accordingly, the governing equation of motion for the cable

TABLE 1: Power Line Parameters

Parameter		Value
Mass	m	0.68 kg
Length	L	3.66 m
Tension	T	395 N
Diameter	d	1.05×10^{-2} m
Flexural Rigidity	EI	40.8 m^4

can be written as

$$EIy'''' + m\ddot{y} + Ty'' = F(x,t) - (F_1 + F_2)D(x) \tag{1}$$

In the above equation $F(x,t)$ is an excitation force at a single point and can be expressed as

$$F(t) = f_0 sin(\omega_e t) \tag{2}$$

where f_0 is the amplitude of the force, and ω_e is the excitation frequency. Further, F1, F2 and D(x) are expressed as

$$F_1 = m_d\ddot{y} \tag{3}$$

$$F_2 = k(y - y_d) + c(\dot{y} - \dot{y_d}) \tag{4}$$

$$D(x) = \delta(x - x_r) \tag{5}$$

The governing equation of motion for the suspended mass is given by

$$m_d\ddot{y}_d - F_2 = 0\,. \tag{6}$$

For this paper, the standalone powerline will be considered. A numerical model is built and the data from this model will be used for the paper. Two models will be considered, one where the span is split into 20 elements while the other model has the span split into 100 elements.

2.1 Data Driven Modeling

The method used in this paper is Dynamic Mode Decomposition (DMD) [12–14]. It is a technique for modeling complex dynamical systems using time-series data. DMD decomposes the time-series data into a set of spatial modes and their temporal frequencies and can capture the dynamics of the system. The system under consideration is assumed to obey the following discrete-time model.

$$X^m_{k+1} = AX^m_k \tag{7}$$

, where

$$X_k = \begin{bmatrix} | & | & & | \\ x_1 & x_2 & x_3 \cdots & x_m \\ | & | & & | \end{bmatrix} \tag{8}$$

and

$$X_{k+1} = \begin{bmatrix} | & | & & | \\ x_2 & x_3 & x_4 \cdots & x_{m+1} \\ | & | & & | \end{bmatrix} \tag{9}$$

X is a collection of states of previous time steps as column vectors and k denotes time steps. m is the order of the system which is the number of column vectors in X (ie number of previous time step data under consideration as shown in (8) and (9).

The matrix A is the operator that maps X_k to X_{k+1} which essentially makes it a state-transition matrix like in state space models. Since the state vectors are not invertible, we resort to the Moore-Penrose pseudo-inverse. The Moore-Penrose pseudo-inverse is a generalization of the matrix inverse for non-square

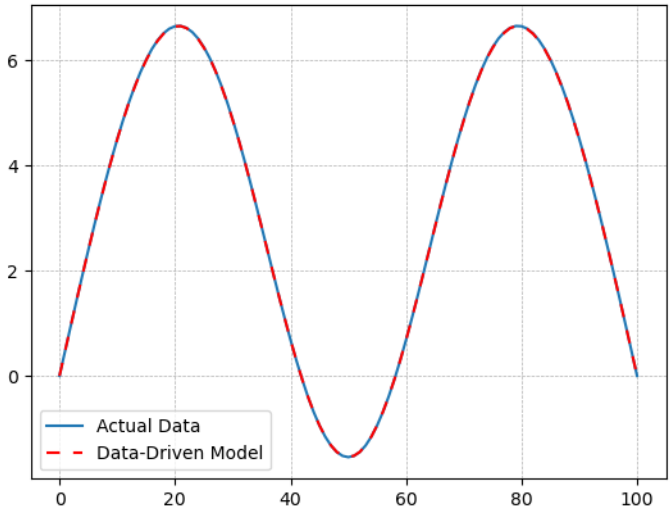

FIGURE 3: State Transition Matrix

and singular matrices. Given a matrix A, its pseudo-inverse denoted as A^+ is unique and satisfies the following properties:

$$\begin{aligned} A\left(A^+\right)A &= A \\ \left(A^+\right)A\left(A^+\right) &= A^+ \\ \left(A\left(A^+\right)\right)^* &= A\left(A^+\right) \\ \left(\left(A^+\right)A\right)^* &= \left(A^+\right)A \end{aligned} \tag{10}$$

, where $*$ represents the conjugate transpose operation. When a linear system $Ax - b$, has no exact solution, the pseudo-inverse can be used to find the least squares solution. The vector $x = A^+b$ minimizes the Euclidean norm of the residual $|Ax - b|$.

So, the state-transition matrix can be approximated as:

$$A \approx X_{k+1}X_k^+ \tag{11}$$

As seen in figure fig. 3, it is evident that A is a good approximation of the state-transition matrix.

2.2 Stability of the system

To analyze the stability of the system, the eigenvalues of A are studied. The eigenvalues denoted as λ_i give insight into the temporal behavior and stability of the system. In a discrete-time system, the system is stable if all the eigenvalues fall within the unit circle in the complex plane i.e.:

$$|\lambda_i| < 1 \forall i \in 1, 2, \ldots, r \tag{12}$$

where r is the number of modes. If any eigenvalue has a magnitude greater than or equal to 1, the corresponding mode will grow exponentially over time, indicating unstable behavior. Eigenvalues with magnitudes of less than 1 correspond to stable modes that decay over time.

In fig. 4, the maximum values of the imaginary and real parts are 114.98 and 663.46. Out of 101 eigenvalues, 11 are outside the unit circle and these eigenvalues correspond to modes that will grow exponentially. This means that our system behavior

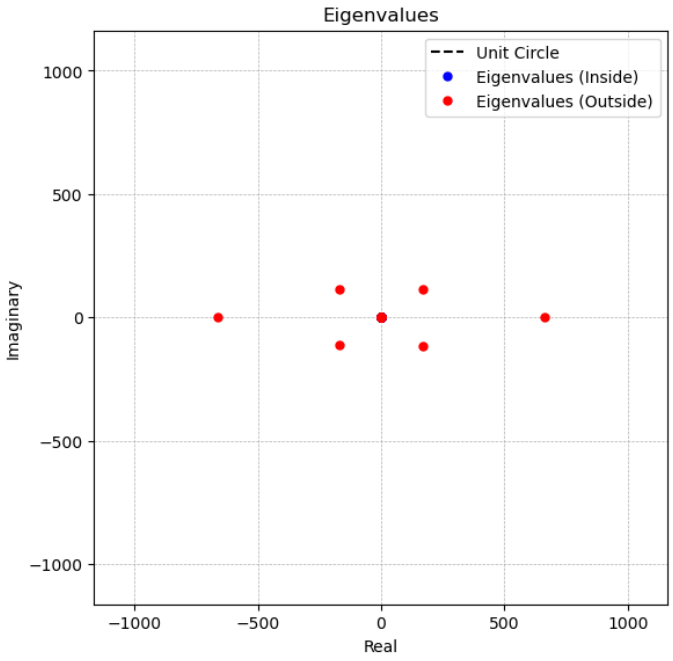

FIGURE 4: System Afer DMD

will also grow exponentially and hence it is unstable. So, the system has to be stabilized while making sure that A is still a good approximation of the state-transition matrix.

2.3 Tikhonov Regularization

Tikhonov Regularization modifies the problem by adding a regularization term to the objective function, [15, 16]. The regularized objective function then becomes:

$$\min_A |X_{k+1} - AX_k|_F^2 + \alpha|A|_F^2 \tag{13}$$

where $\alpha > 0$ is the regularization parameter, $|\cdot|_F$ denotes the Frobenius norm. The regularization term $\alpha|A|_F^2$ penalizes large values in the matrix A, promoting stability. Then the regularized state-transition matrix, A_{reg} can be calculated as:

$$A_{reg} = X_{k+1}X_k^T(X_kX_k^T + \alpha I)^{-1} \tag{14}$$

where I is the identity matrix.

In fig. 5, the maximum values of the imaginary and real parts are 0.1212 and 0.9868 respectively. All the eigenvalues lie within the unit circle and hence the system is stable. As seen in fig. 6, A_{reg} is still a good approximation of the state-transition matrix. The choice of the regularization parameter, λ is crucial for achieving the perfect balance in A_{reg}. A larger value of λ will push the eigenvalues to the origin thus improving stability, but if λ is too large the resulting A_{reg} may not be able to accurately capture the dynamics of the system.

2.4 Kalman Filter

The Kalman Filter operates on the principle of prediction and correction and follows a two-step process that first predicts

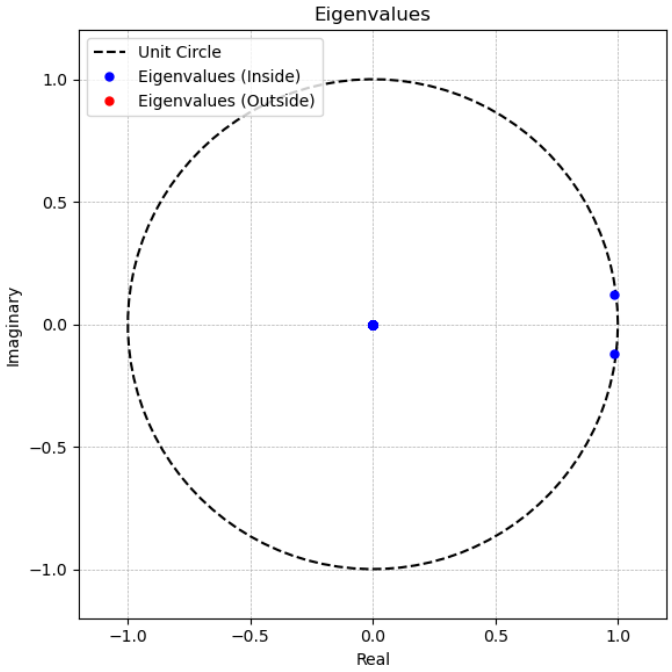

FIGURE 5: System after DMD and Regularization ($\alpha = 0.1$)

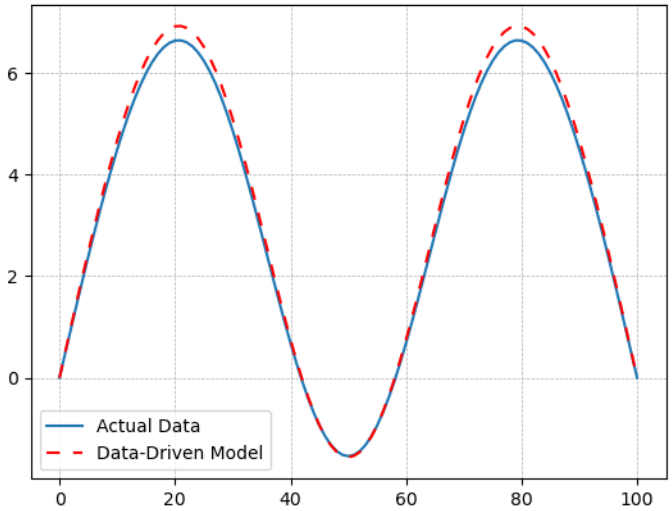

FIGURE 6: State Transition Matrix after Regularization

the system's future states and then corrects the prediction based on new measurement data, [17]. This allows the filter to estimate the states in real time and it can also predict all the states of the system even when the system is only partially observable. This paper implements a tailored Kalman Filter to work with the data-driven workflow. The filter works as follows:

Prediction:

$$\hat{x}_{k|k-1} = A\hat{x}_{k-1|k-1} + Q \tag{15}$$

$$P_{k|k-1} = AP_{k-1|k-1}A^T + Q + \varepsilon I \tag{16}$$

where $\hat{x}$ is the state vector
q is the process noise
P is the covariance matrix

Update:

$$y_k = z_k - H_k\hat{x}_{k|k-1} \tag{17}$$

$$S_k = H_{k|k-1}H^T + R + \varepsilon I \tag{18}$$

$$K_k = P_{k|k-1}H^T S_k^{-1}\hat{x}_{k|k} = \hat{x}_{k|k-1} + K_k y_k \tag{19}$$

$$P_{k|k} = (I - K_k H)\, P_{k|k-1} \tag{20}$$

where:
z is the new measurement data
y is the measurement residual
S is the innovation covariance
K is the Kalman Gain
R is the measurement noise
ε is the regularization term

The regularization term ε is a small value and ensures the numerical stability of the Kalman Filter, [18]. Adding a small value to the innovation covariance will prevent it from approaching singularity. Also, this implementation of the Kalman Filter assumes that only the first few states in the system are observable.

3. RESULTS AND DISCUSSION

This section discusses the results and performance of the Kalman Filter.

3.1 20 Element Model

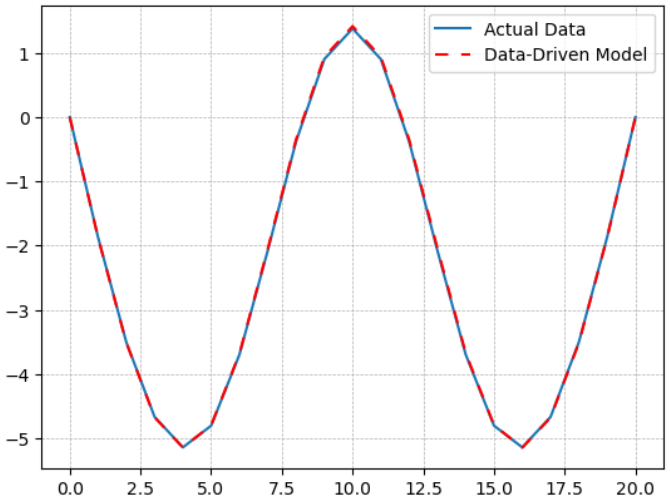

FIGURE 7: Performance of KF on 20 Element Model: $\varepsilon = 1$

Total number of states: 21
Number of observable states: 10

Fig. 7 shows the performance of the Kalman Filter on the 20-element model. The filter can accurately track all 21 states in the system using the measurements from the first 10 states.

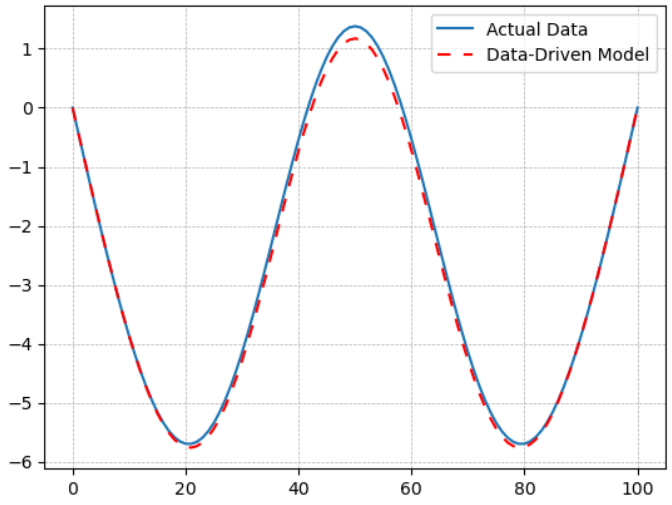

FIGURE 8: Performance of KF on 100 Element Model: $\varepsilon = 1$

3.2 100 Element Model

Total number of states: 101
Number of observable states: 13

Fig. 8 shows the performance of the Kalman Filter on the 100-element model. The filter can accurately track all 101 states in the system using the measurements from the first 13 states.

4. CONCLUSION AND FUTURE WORK

This paper demonstrated that the use of DMD to model the dynamics combined with Tikhonov Regularization to stabilize the system and a Kalman Filter for state estimation is a viable alternative to numerical methods. The estimations from the filter agree with the numerical simulation. This method will also be able to adapt to changes in the dynamics of the system(i.e. the powerline) since the dynamics is captured using data from the system. Another interesting find is that even though the number of states increased from 21 to 101 between the two models under consideration, the number of observable states required for accurate state estimation has not changed much.

Further research is needed into better methods of updating the state transition matrix over time. The time delay with which the filter can accurately estimate states during sudden changes in dynamics is also to be studied. Also, in this paper, the first few states are considered to be observable, and more research is required to find the optimal distribution of observable states along the span of the powerline.

REFERENCES

[1] Barry, Oumar, Oguamanam, Donatus and Lin, Der. "Aeolian vibration of a single conductor with a Stockbridge damper." Vol. 227: pp. 935–945. 2013.

[2] Barry, Rafiou Oumar. "Vibration Modeling and Analysis of a Single Conductor With Stockbridge Dampers." Ph.D. Thesis, University of Toronto. 2014.

[3] Braga, GE, Nakamura, R and Furtado, TA. "Aeolian vibration of overhead transmission line cables: endurance limits.": pp. 487–492. 2004.

[4] Barry, Oumar and Bukhari, Mohammad. "On the modeling and analysis of an energy harvester moving vibration absorber for power lines." Vol. 58288: p. V002T23A005. 2017.

[5] Barry, Oumar Rafiou, Tanbour, Emadeddin Y, Vaja, Nitish Kumar and Tanbour, Hesham. "Asymmetric Aeolian vibration damper." (2017).

[6] Rezaei, A and Sadeghi, MH. "Analysis of aeolian vibrations of transmission line conductors and extraction of damper optimal placement with a comprehensive methodology." *International Journal of Engineering* Vol. 32 (2019): pp. 328–337.

[7] Kakou, Paul, Bukhari, Mohammad, Wang, Jiamin and Barry, Oumar. "On the vibration suppression of power lines using mobile damping robots." *Engineering Structures* Vol. 239 (2021): p. 112312.

[8] Kakou, Paul. "Towards A Mobile Damping Robot For Vibration Reduction of Power Lines." (2021).

[9] Kakou, Paul-Camille and Barry, Oumar. "Toward A Mobile Robot for Vibration Control and Inspection of Power Lines." *ASME Letters in Dynamic Systems and Control* Vol. 2 (2021): p. 011001.

[10] Bukhari, Mohammad A and Barry, Oumar R. "Nonlinear Vibrations Analysis of Overhead Power Lines: A Beam With Mass–Spring–Damper–Mass Systems." *Journal of Vibration and Acoustics* Vol. 140 (2018).

[11] Choi, Andrew. "Investigation of a Mobile Damping Robot for Electric Transmission Lines." (2023).

[12] SCHMID, PETER J. "Dynamic mode decomposition of numerical and experimental data." *Journal of Fluid Mechanics* Vol. 656 (2010): p. 5–28. DOI 10.1017/s0022112010001217.

[13] ROWLEY, CLARENCE W., MEZIĆ, IGOR, BAGHERI, SHERVIN, SCHLATTER, PHILIPP and HENNINGSON, DAN S. "Spectral analysis of nonlinear flows." *Journal of Fluid Mechanics* Vol. 641 (2009): p. 115–127. DOI 10.1017/s0022112009992059.

[14] Kutz, J Nathan, Brunton, Steven L, Brunton, Bingni W and Proctor, Joshua L. *Dynamic mode decomposition: data-driven modeling of complex systems*. SIAM (2016).

[15] Hansen, Per Christian. "Analysis of Discrete Ill-Posed Problems by Means of the L-Curve." *SIAM Review* Vol. 34 No. 4 (1992): pp. 561–580. DOI 10.1137/1034115.

[16] Tikhonov, A. N., Goncharsky, A. V., Stepanov, V. V. and Yagola, A. G. *Algorithms and programs for solving linear ill-posed problems*. Springer Netherlands (1995): p. 97–161. DOI 10.1007/978-94-015-8480-7_5.

[17] (2006). DOI 10.1002/0470045345.ch13. URL http://dx.doi.org/10.1002/0470045345.ch13.

[18] Miller, B.M. and Rubinovich, E.Ya. "Regularization of a generalized Kalman filter." *Mathematics and Computers in Simulation* Vol. 39 No. 1–2 (1995): p. 87–108. DOI 10.1016/0378-4754(95)00024-r.

[19] Barry, O, Zu, JW and Oguamanam, DCD. "Forced vibration of overhead transmission line: analytical and experimental investigation." *Journal of Vibration and Acoustics* Vol. 136 (2014).